# Comparison of Thin-Layer and Bulk MIPs Synthesized by Photoinitiated *In Situ* Crosslinking Polymerization from the Same Reaction Mixtures

**Frank Schneider,[1] Sergey Piletsky,[2] Elena Piletska,[2] Antonio Guerreiro,[2] Mathias Ulbricht[1]**

[1]*Lehrstuhl für Technische Chemie II, Universität Duisburg-Essen, 45117 Essen, Germany*
[2]*Institute of BioScience and Technology, Cranfield University, Silsoe, Bedforshire, MK45 4DT, United Kingdom*

Received 10 June 2004; accepted 26 January 2005
DOI 10.1002/app.22112
Published online in Wiley InterScience (www.interscience.wiley.com).

**ABSTRACT:** The synthesis and comparative characterization of molecularly imprinted polymers (MIPs) in two different formats, as thin layers grafted to the entire surface of polypropylene microfiltration membranes and as conventional particles, are described. Imprinting with atrazine was performed by using itaconic acid and *N*,*N*′-methylene-bisacrylamide as functional and crosslinker monomers in methanol as the solvent. Polymerization had been initiated by UV irradiation of benzoin ethyl ether and driven to low monomer conversion for the thin-layer polymers and to high monomer conversion for the bulk materials. The binding performance of MIP composite membranes and of MIP particles packed into cartridges was evaluated in solid-phase extraction (SPE) experiments of atrazin and simazin from aqueous solutions. The SPE performance depended strongly on pH and buffer concentration. Although an imprinting effect was observed for both formats, the specificity (MIP versus Blank) and the selectivity (atrazin versus simazin) were much higher for the thin-layer composite membranes than for the bulk polymer particles. In particular, the atrazin/simazin selectivity increased from 32% for the Blank to 78% for the MIP composite membranes. A major reason is the hindered accessibility of the internal pore structure of the particles, whereas the porous filtration membranes are much more compatible with the fast SPE protocol. Furthermore, based on $pK_a$ of the functional carboxylic acid groups—from potentiometric titration and polarity of the binding environment—from fluorescent probe analysis, different properties of the imprinted binding sites can be postulated for the two MIP formats. However, the differences between MIP and Blank were much more pronounced for the thin-layer composite membranes. The hydrophobic surface of the polypropylene membrane appeared to be a major factor affecting the binding performance of thin-layer MIPs. The new porous composite membranes could be particularly useful as selective SPE materials in environmental, pharmaceutical, and analytical applications. © 2005 Wiley Periodicals, Inc. J Appl Polym Sci 98: 362–372, 2005

**Key words:** crosslinking; molecular imprinting; nanotechnology; photopolymerization; surfaces

## INTRODUCTION

Molecularly imprinted polymers (MIPs) can be prepared by the copolymerization of functional and crosslinker monomers in the presence of a template molecule.[1] The noncovalent synthesis of MIPs is the easiest and most straightforward approach.[1,2] After removal of the template, the imprints retain the position of the functional groups and have a shape complementary to the template. Commonly, MIPs prepared in bulk by using a large excess of crosslinker monomer are finely ground, sieved, washed, and used as particles.[1,2] The process is tedious and often results in large losses of the material (including template) as fines. In addition, it is often complicated to interpret and optimize the binding properties of bulk MIP materials because the macro- and micropore morphology as well as the nanosized imprinted binding sites are formed from the same building blocks (monomers) simultaneously. All this explains the growing interest in alternative formats of MIP preparation. Thin MIP films, especially those on suited supports, and MIP composite membranes are especially attractive.[3]

For the preparation of thin films by *in situ* crosslinking polymerization, either a selective initiation of the reaction in a thin layer adjacent to the support surface or/and the grafting-from a support material are the most promising approaches. Examples for such attempts included spin-coating thin layers of the reaction mixture on an inert plane substrate and subsequent UV-initiated polymerization[4] or using polymerization initiators covalently immobilized on porous silica surface for the initiation of grafting-from crosslinking polymerization.[5] The controlled photoinitiated grafting of thin-layer MIPs to surfaces of either plane substrates or porous supports[6–8] offers many possibilities for the development of novel composite materials for affinity technologies. One important conclusion from the previous work was that a low thick-

Correspondence to: M. Ulbricht (mathias.ulbricht@uni-essen.de).


© 2005 Wiley Periodicals, Inc.

ness of grafted MIP layers, typically in the range of a few to ~-15 nm, provides optimum imprinting effect[3] (i.e., high rates and efficiencies for adsorption-desorption of the template). Thin polymer layers should also reduce the template leaching, which is very important for pharmaceutical applications of MIP-based materials for solid phase extraction (SPE). Furthermore, for grafting, the content of crosslinker monomer required to achieve the highest specificity was lower than required for bulk preparations. That might be especially beneficial for imprinting of large molecules.[6–8]

Thin-layer MIP composite membranes based on microfiltration membranes, with high permeabilities and binding capacities, could ultimately be the perfect solution for high-performance affinity SPE.[3,6–9] However, to achieve this goal, it would be necessary to gain a better understanding of the grafting process influencing MIP synthesis and performance. It would be particularly important to understand to what degree the large, and often empirical, knowledge about syntheses and properties of conventional bulk MIPs can be related to the thin-layer MIPs.

This work is the first comparative study of the influence that polymerization conditions exert on the MIP recognition properties, performed for two different systems yielding different MIP formats: thin polymeric films grafted to the entire surface of microfiltration membranes and bulk polymer particles. The same reaction mixtures for imprinting the template atrazine—a triazine herbicide—had been used under conditions that had been adapted to the respective format. Thus, obtained porous thin-layer composite membranes based on polypropylene and bulk polymer particles had been evaluated under SPE conditions for estimating the MIP specificity (atrazine binding of MIP versus Blank) and selectivity (atrazine versus simazin) (Schemes 1 and 2).

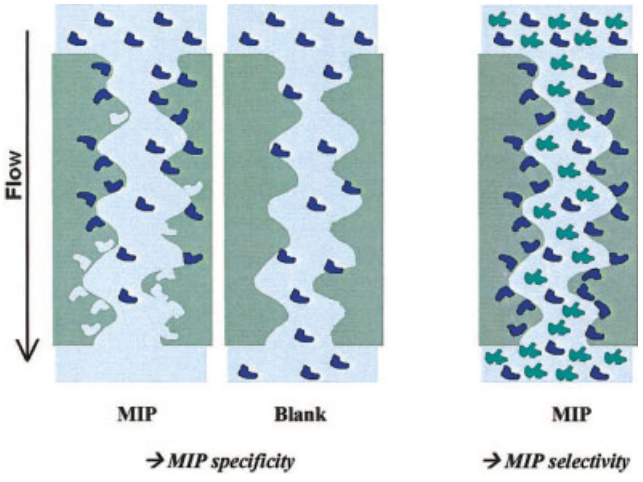


**Scheme 1** Schematic description of SPE experiments towards characterization of MIP specificity (binding of the template by MIP versus Blank) and selectivity (competitive binding of the template and another substance to the MIP or Blank).

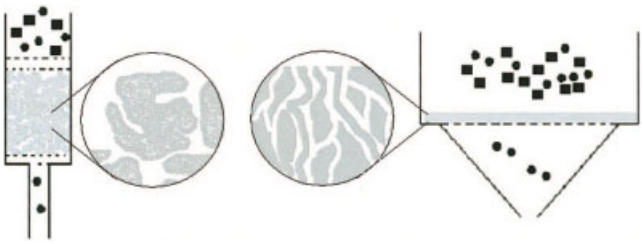

**Scheme 2** Separation unit formats for SPE evaluation of polymer particles (left) and porous composite membranes (right); the squares should symbolize a substance that is specifically bound by the adsorber material while another substance such as the one symbolized with the circles would pass the adsorber bed unbound. (Note that in the experiments the particle diameter was between 25 and 45 $\mu$m, whereas the characteristic pore diameter of the membrane was $<1$ $\mu$m.)

## EXPERIMENTAL

### Materials

Polypropylene (PP) microfiltration membranes (2E HF) with a cut-off pore diameter of 0.4 $\mu$m and a thickness of 155 $\mu$m were purchased from Membrana GmbH (Wuppertal, Germany). Itaconic acid (IA, Aldrich), *N*,*N*′-methylene-bisacrylamide (MBAA, Aldrich), benzoin ethyl ether (BEE, Aldrich, München, Germany), atrazine and simazine (PESTANAL®, Riedel de Haën, München, Germany), and dansyl chloride (Sigma, München, Germany) were used as received without further purification. Methanol, acetonitrile, acetone (all HPLC grade), and buffer salts (for analysis) were used for polymer preparations and characterizations.

### Preparations and characterizations

#### Syntheses

The reaction mixtures for MIP syntheses contained 2.5 mM photoinitiator (BEE), 300 mM crosslinker (MBAA), 50 mM functional monomer (IA), and 10 mM template (atrazine) dissolved in methanol. Blank materials were prepared by using the same mixture but without atrazine.

Surface functionalization was performed according to the already described general procedure.[8] Briefly, the membranes were first precoated with BEE and then immersed in the reaction mixture, and after 1 min, UV irradiation was performed with a UV A Print 100 lamp (Dr. Hönle AG, Gräfelfing, Germany). Washing for 15 min and Soxhlet extraction with methanol for at least 4 h followed. The degree of grafting (DG) was determined gravimetrically. In preliminary experiments, the UV time had been varied and the DG

determined; in parallel, the BEE conversion had been monitored by UV spectroscopy (330 nm).

For bulk polymer preparation, the reaction mixture was filled into a 20-mL screw-cap vessel, which was then closed, put in an ice bath, and UV irradiated for 20 min with a Collimated Xenon ARC lamp LX300F (Cermax©, Perkin Elmer Optoelectronics, Fremont, CA). After polymerization, the bulk polymer was ground by using an electric mortar (SL2, Silverson, East Longmeadow, MA), followed by a sieving. The fraction with particle sizes 25–45 $\mu$m was collected and washed with methanol and 1 g polymer suspension was packed into a HPLC column for continuous washing with methanol, 100 mM HCl in methanol, and water/methanol 85/15 (v/v).

*Pore structure characterization*

The specific surface area ($S_{\text{spec}}$) was determined by using the surface area analyzers SA 3100 (Beckman-Coulter GmbH, Krefeld, Germany) for the composite membranes and Nova 1000e (Quantachrom Corp., Syosset, NY) for the bulk particles.

Volume swelling, porosity of the bulk particles, as well as the interstitial volume of the particle bed were determined by analyzing the volume and mass increase relative to the dry state. Particles were filled into a graduated test tube (d $\sim$ 6 mm) and shaken by using a Vortex tube mixer until a dense particle bed of 250 $\mu$L ($V_{\text{bed,dry}}$) had been obtained. Then, the weight ($m_{p,\text{dry}}$) was also measured. Thereafter, 1.5 mL water was added, the bed volume ($V_{\text{bed,sw}}$) was measured after equilibration for 24 h, and the relative volume swelling ($SW$) was calculated according to:

$$\text{SW} = \frac{V_{\text{bed,sw}} - V_{\text{bed,dry}}}{V_{\text{bed,dry}}} 100\% \quad (1)$$

Particles were weighed in a test tube ($m_{p,\text{dry}}$) and then swollen to equilibrium in water. To remove the water from the interstitial volume, the test tube was closed with a plug of cellulose, turned upside down, and centrifuged at 1200 min$^{-1}$ for at least 5 min. Then, the particles filled with water in the pores were weighed again ($m_{sw}$). The volume porosity ($P$) of the particles in the swollen state was calculated according to:

$$P = \frac{(m_{\text{sw}} - m_{P,\text{dry}})/\rho_{\text{H}_2\text{O}}}{m_{P,\text{dry}}/\rho_P + [(m_{\text{sw}} - m_{P,\text{dry}})/\rho_{\text{H}_2\text{O}}]} 100\% \quad (2)$$

with $\rho_p$ as the polymer density and $\rho_{\text{H2O}}$ as the density of water.

The relative interstitial volume ($IV$) of a particle bed could then also be estimated assuming that the degree of swelling will not be influenced by the kind or size of housing:

$$IV = \frac{V_{\text{bed,sw}} - (m_{P,\text{dry}}/\rho_P) + [(m_{\text{sw}} - m_{P,\text{dry}}/\rho_{H_2O})}{V_{\text{bed,sw}}} 100\% \quad (3)$$

pK$_a$ determination using potentiometric titration

A pH-meter (Hanna Instruments 8519, Deutschland GmbH, Kehlam Rhein, Germany) was used to monitor the titration of polymeric functional groups. Two membranes ($d$ = 4.6 cm) were soaked in methanol for 2 min before immersing them into a beaker filled with distilled water. NaOH solution (0.1$M$) was used to adjust a pH value to 12. Hydrochloric acid (0.1$M$) was added drop-wise (8 $\mu$L) until a pH value of 2 was achieved. The waiting time between the drops at the beginning was 2 min. To consider the problems of pore diffusion, the waiting time in the critical pH area was increased to 30 min between the drops. Approximately 0.3 g of bulk particles was used for the pK$_a$ determination in the same way as described above.

Binding site characterization by reflection fluorescence experiments

The membranes were soaked for 2 h under light exclusion in 10 mL of a solution made from a mixture (20/80, v/v) of a solution of dansyl chloride (15 mg/L) in acetone and a solution of sodium carbonate (2$M$, pH 11.0). After the soaking time, they were rinsed with acetone for 5 min to remove nonspecifically bound dye. Then the membranes were immersed in water and analyzed by using a Reflection fluorescence spectrometer (Fluoromax 2, Spex, HORIBA Jobin Yvon Ltd., Stanmore, Middlesex, UK). Bulk particles (20 mg) were equilibrated in the same solution as the one described above. After the incubation, the polymer was washed with acetone, dried at 60°C and suspended in water, and analyzed by using a Spectrofluorometer (RF 5001 PC, Shimadsu, Deutschland GmbH, Duisburg, Germany). The excitation wavelength for the membrane and particle characterization was 330 nm and the emission maximum was detected between 450 and 550 nm.

SPE evaluation

Membrane solid-phase extractions were performed by using a syringe connected to a 25-mm-diameter filter holder (Swinnex™, Millipore GmbH, Eschborn, Germany) containing one membrane (effective membrane area, 4 cm$^2$). Bulk solid phase extractions were performed by using a syringe connected to a 1-mL PP cartridge (Preppy™, Supelco, Sigma-Aldrich Chemie GmbH, München, Germany) with a 0.22-$\mu$m frit which had been loaded with 15-mg particles. In both cases, 10 mL of $10^{-5}M$ atrazine solution in potassium dihydrogen phosphate (pH 5–8) or glycine (pH 3.5) buffer was filtered through the SPE unit at a rate of 10 mL/min. The concentration of atrazine in the feed and in the permeate was determined by using a HPLC system (Kontron Instruments Ltd., Bletchley, UK) on a Phenomenex Luna C18 (3 $\mu$m, 150 $\times$ 3 mm) column

with a flow rate of 0.3 mL/min of the mobile phase (acetonitrile-ammonium dihydrogenphosphate 70/30, v/v). The detection was performed spectrophotometrically at 220 nm. For selectivity measurements, an atrazine-simazine solution (both in $10^{-5}M$ concentration) was used. The selectivity ($S$) was calculated according to:

$$S = \left(\frac{n_{a,f}}{n_{s,f}} - \frac{n_{a,p}}{n_{s,p}}\right)100\% \quad (4)$$

with $n_{a,f}$ ($n_{s,f}$) amount of atrazine (simazine) in the feed, $n_{a,p}$ ($n_{s,p}$) amount of atrazine (simazine) in the permeate. The average measuring error of all SPE measurements was below 10%.

## RESULTS AND DISCUSSION

### Syntheses

The aim of this work was to compare binding and recognition properties of thin-layer and bulk MIPs prepared via *in situ* polymerization from the same reaction mixtures. Because thin-layer MIP composite membranes had already been successfully prepared for SPE from aqueous solutions, the focus of this study was also on MIP function and evaluation under aqueous conditions. The functional monomer selected was IA, which according to molecular modeling results should provide a good affinity towards atrazine.[10] The choice of crosslinker—MBAA—and solvent—methanol—was determined by the solubility of the components and the necessity to achieve the water compatibility of the polymers. In particular, MIPs should have similar swelling under preparation and operation (here SPE) conditions.[11] MBAA had been used successfully for the synthesis of thin-layer MIPs for aqueous SPE.[6–8] Also, MBAA had recently been used for the synthesis of bulk MIPs; both synthesis and evaluation had been done in aqueous solutions.[12] Furthermore, it had been suggested that more hydrophilic functional and/or crosslinker monomers will reduce the nonspecific adsorption due to hydrophobic bonding in water, and that those monomers will thus contribute to an increased MIP specificity.[13] The crosslinker/functional monomer molar ratio (6 : 1) had been selected between typical bulk MIP synthesis conditions (up to 10 : 1[1,2]) and the ratios identified as optimal for the synthesis of thin-layer MIPs (between 5 : 1[7] to 2 : 1[6]). Recently, other groups had also reported about hydrophilic bulk MIPs obtained with very low crosslinker/functional monomer ratios, such as, for example, 1 : 1.[12,14]

While during conventional bulk MIP syntheses the final degree of monomer conversion is very high, the preparation of thin-layer MIPs had been achieved at very low degrees of monomer conversion in the reaction mixture, used for a mainly heterogenous copolymerization.[8] In addition, the confinement of the photoinitiator on the surface of the support material by preadsorption had been proven to be essential for obtaining a significant MIP specificity.[8] Therefore, it seemed possible, by using the same initiator, that the $\alpha$-scission photoinitiator BEE yielded alkyl and acyl starter radicals[8] for both bulk and thin-layer syntheses.

By photoinitiation of the thin-layer MIP functionalization of the PP microfiltration membranes, the DG could be adjusted by the UV irradiation time (Fig. 1). In the investigated range, the DG correlated with the photoinitiator conversion. For further evaluation, MIP and Blank composite membranes with a DG around 500 $\mu g/cm^2$ had been selected and could be reproducibly synthesized by using a UV irradiation time of 2.0 min. This corresponded to a degree of monomer conversion of about 7%, and the gelation point for the reaction mixture had not yet been reached (under these conditions, gelation had been observed at $\sim 3$ min; data not shown).

For the bulk syntheses, reaction conditions should be as similar as possible to the thin-layer grafting. Bulk polymerizations at longer reaction times towards higher degrees of monomer conversion will inevitably result in significant heat generated by the exothermic nature of the reaction. The increase of temperature could weaken the electrostatic interactions between the functional monomers and the template molecules.[15] Hence, the bulk polymerizations were performed by using an ice bath for external cooling to ensure that the maximal polymerization temperature would not rise above the temperature generated during the grafting. An UV irradiation time of 20 min had been found to yield a maximum polymer yield (always at more than 80% monomer conversion), even when the photoinitiator conversion was still about only 80%. The reason for the apparently higher polymerization efficiency of the bulk syntheses—as expressed by the ratio of polymer yield versus photoinitiator conversion (cf. Fig. 1)—was presumably that the grafting reaction had been stopped at a such low degree of conversion (and before gelation, cf. above) so that oligomer or very weakly crosslinked polymer products could still be extracted. To yield a homogeneous particle size distribution, the bulk polymer had to be ground and sieved.

To compare the SPE binding capability of composite membranes and bulk particles, their surface area was measured by nitrogen adsorption (based on the BET model according to Brunauer, Emmet and Teller). The specific surface area data for membranes grafted with Blank or MIP were all between 19 and 23 $m^2/g$; these values were not significantly different from the data for the unmodified membrane determined earlier (23 $m^2/g$[16]). Hence, the PP surface had been covered by a thin polymer layer, and assuming an even coverage of the entire specific surface area of the porous PP mem-

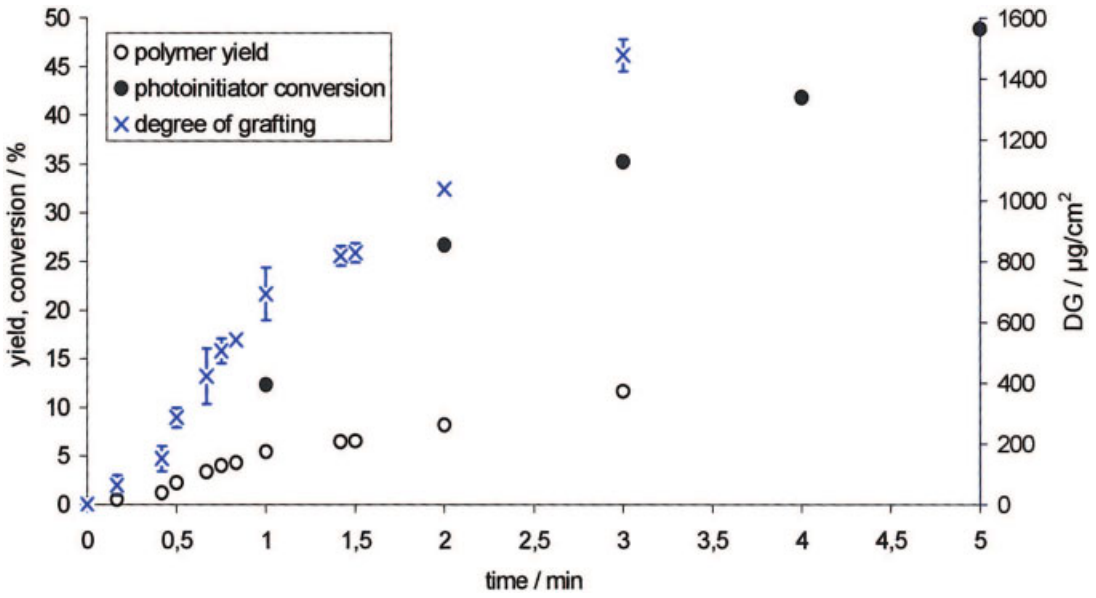


**Figure 1** Degree of grafting (DG) as well as photoinitiator conversion (from UV measurements) and polymer yield (calculated from DG), as a function of UV irradiation time for the functionalization of PP membranes using the monomer mixture of 300 mM MBAA and 50 mM IA in methanol. [Color figure can be viewed in the online issue, which is available at www.interscience.wiley.com.]

brane with a polymer having a density of 1.2 g/cm$^3$, the DG of 500 $\mu$g/cm$^2$ corresponds to a layer thickness of about 6 nm. That the grafted polymer layers on the PP pore walls were indeed very thin had been confirmed by the unchanged water permeabilities of the thin-layer composite membranes as compared with the unmodified PP membranes (not shown). Also, the volume porosity of the PP membranes ($P$ = 76%) remained virtually unchanged after modification (cf. ref. [16]).

The specific surface area data of Blank and MIP prepared in bulk were very similar (Table I). This is evidence that an imprinting effect should not be related to differences in surface area of the polymers and thus to nonspecific binding. The absolute values indicate that the particles had a permanent pore structure. There was an indication for a difference in the volume swelling between MIP and Blank (cf. Table I), what could be explained by a higher overall rigidity of the MIP as compared with the Blank. The swollen state volume porosities of the particles had been estimated by using eq. (2) and assuming a polymer density of 1.2 g/cm$^3$. Rather large values had been obtained (cf. Table I), which can be explained by the hydrophilicity of the crosslinker MBAA. Hence, besides filling the permanent pores of the particles (cf. above), a significant volume fraction of the solvent will be involved in swelling the crosslinked polyacrylamide.

## SPE evaluation

For an even and reproducible contact with the feed solution during SPE, the polymer adsorber bed must be fitted in suited housings. For the thin-layer composite membranes, this problem is solved by tightly fixing the membrane in the filter holder, which provides an even flow distribution through the membrane pores. For the particles, packing of a sufficient quantity (here, 15 mg) in a small SPE cartridge has been used (cf. Scheme 2).

Adsorption measurements started with the analysis of the effect of a pH variation in the sorption solution (Figs. 2 and 3). The bound amounts were much higher for the membranes (Fig. 3) as compared to the particles (Fig. 2). For the bulk particles, the values for MIP and Blank were similar; the adsorbed amounts had a

**TABLE I**
**Morphology Data for Bulk Particles**

| | Specific surface area $S_{spec}$ (m$^2$/g) | Relative volume swelling in water SW (%) | Volume porosity in swollen state $P$ (%) | Relative interparticle volume $IV$ (%) |
|---|---|---|---|---|
| Blank | 61 | $\leq 10$ | 71 | 48 |
| MIP | 62 | $< 5$ | 80 | 54 |

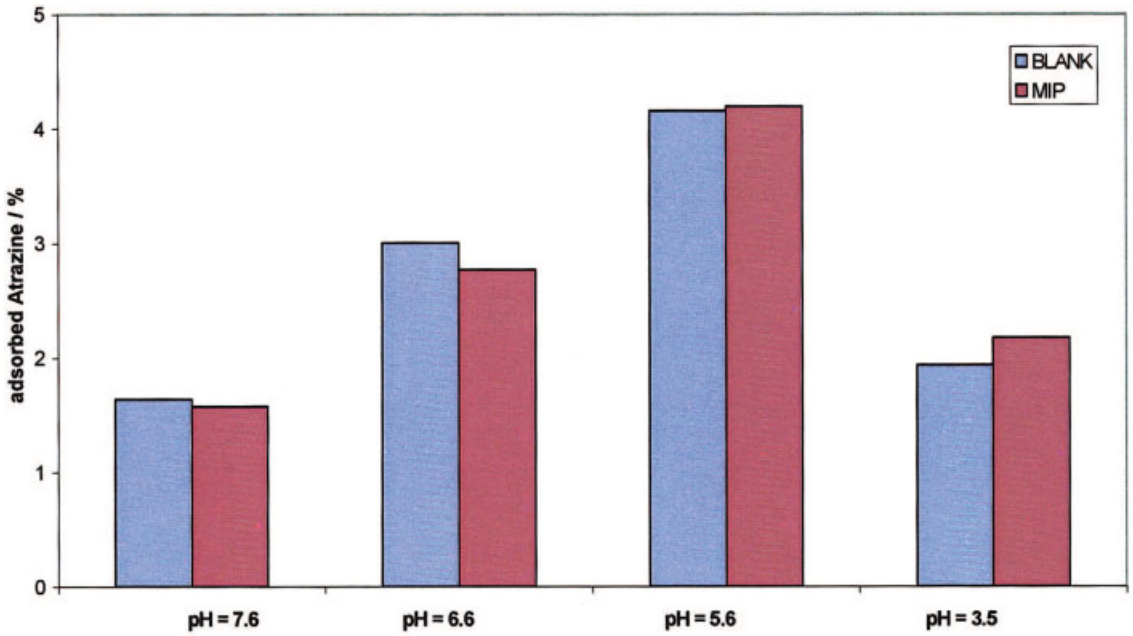


**Figure 2** Binding capacity of bulk particles (300 mM MBAA, 50 mM IA) as a function of pH value ($10^{-5}M$ atrazine, 5 mM buffer), 10 ml/min. [Color figure can be viewed in the online issue, which is available at www.interscience.wiley.com.]

(not very pronounced) maximum at a pH 5.6; a slightly higher binding to the MIP as compared with the Blank could be observed at pH 3.5. For the membranes, the binding to the Blanks clearly decreased with decreasing pH, while the influence of pH on the binding to the MIPs was much less pronounced. At the highest pH, the binding to the Blank was higher; at the lowest pH, an imprinting effect could presumably be identified.

At pH 3.5, where the lowest nonspecific binding to Blanks and an indication of a MIP specificity had been observed, further experiments with varying buffer concentration were performed (Figs. 4 and

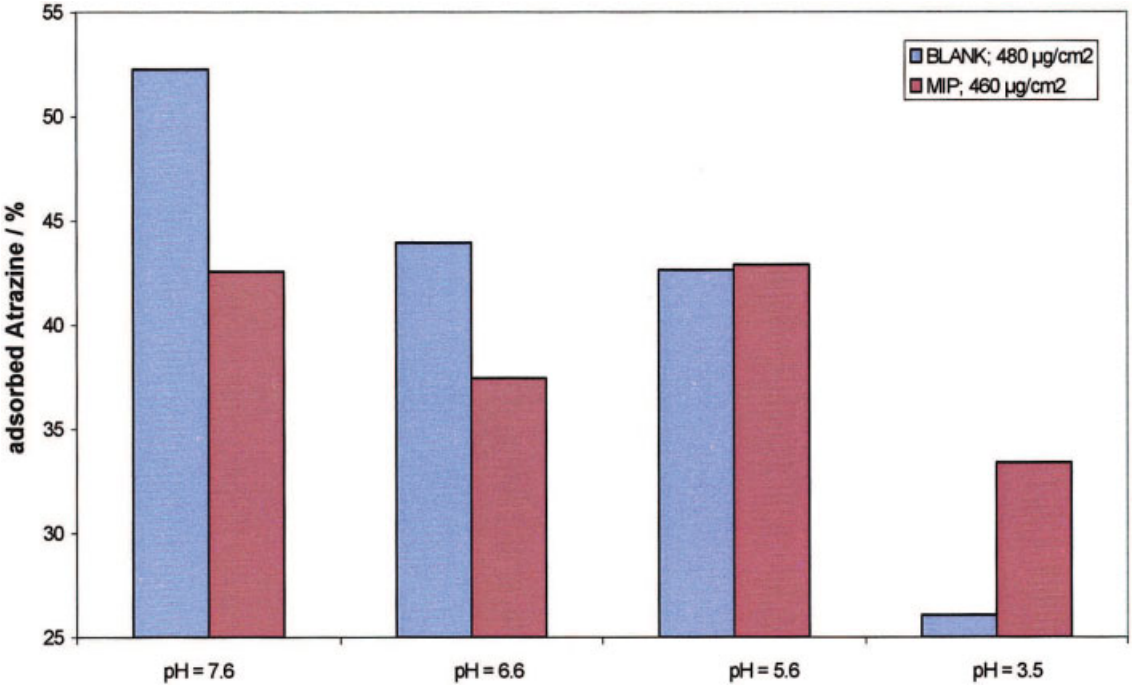


**Figure 3** Binding capacity of thin-layer polymers (300 mM MBAA, 50 mM IA) on PP membranes as a function of pH value ($10^{-5}M$ atrazine, 5 mM buffer), 10 ml/min. [Color figure can be viewed in the online issue, which is available at www.interscience.wiley.com.]

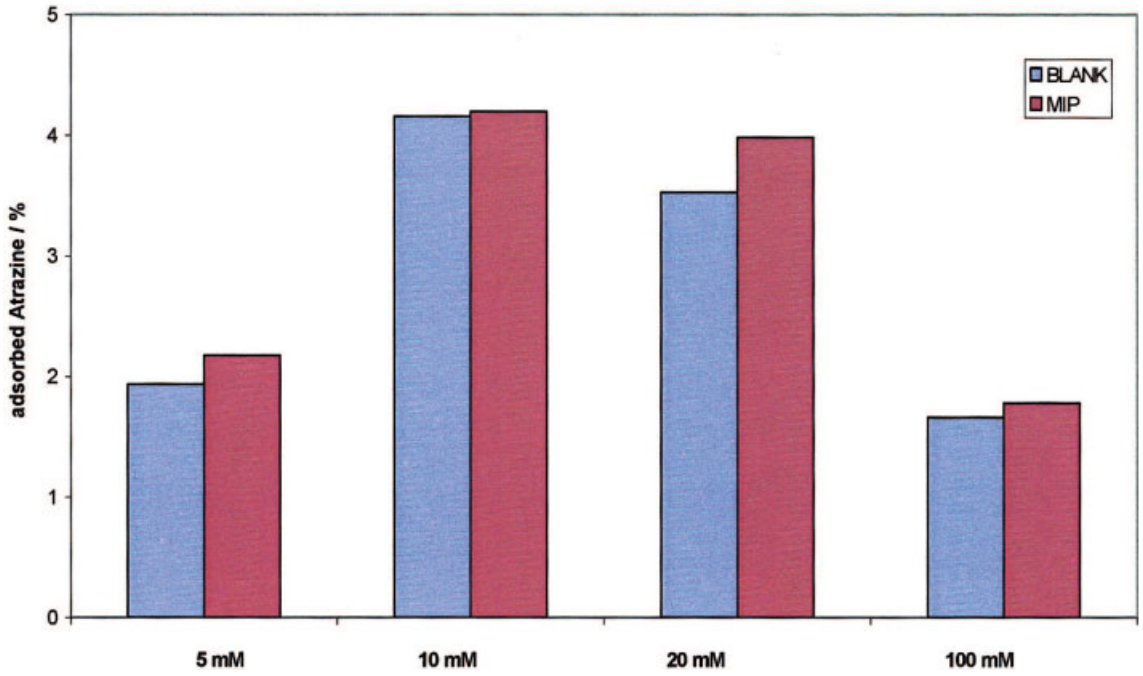


**Figure 4** Binding capacity of bulk particles (300 mM MBAA, 50 mM IA) as a function of buffer concentration ($10^{-5}M$ atrazine, pH 3.5), 10 ml/min. [Color figure can be viewed in the online issue, which is available at www.interscience.wiley.com.]

5). The imprinting effects were confirmed, and the dependence of adsorption capacity on buffer concentration had a maximum for both bulk particles and thin-layer polymers. The thin-layer MIPs showed a much larger imprinting effect than the particles and the maximum was shifted from 20 mM for particles to 100 mM buffer concentration for the membranes.

The selectivity of the polymers was measured by using aqueous feed solutions containing two very similar herbicides—atrazine (2-chloro-4-ethylamino-6-isopropylamino-1,3,5-triazin) and simazine [2-chloro-4,6-

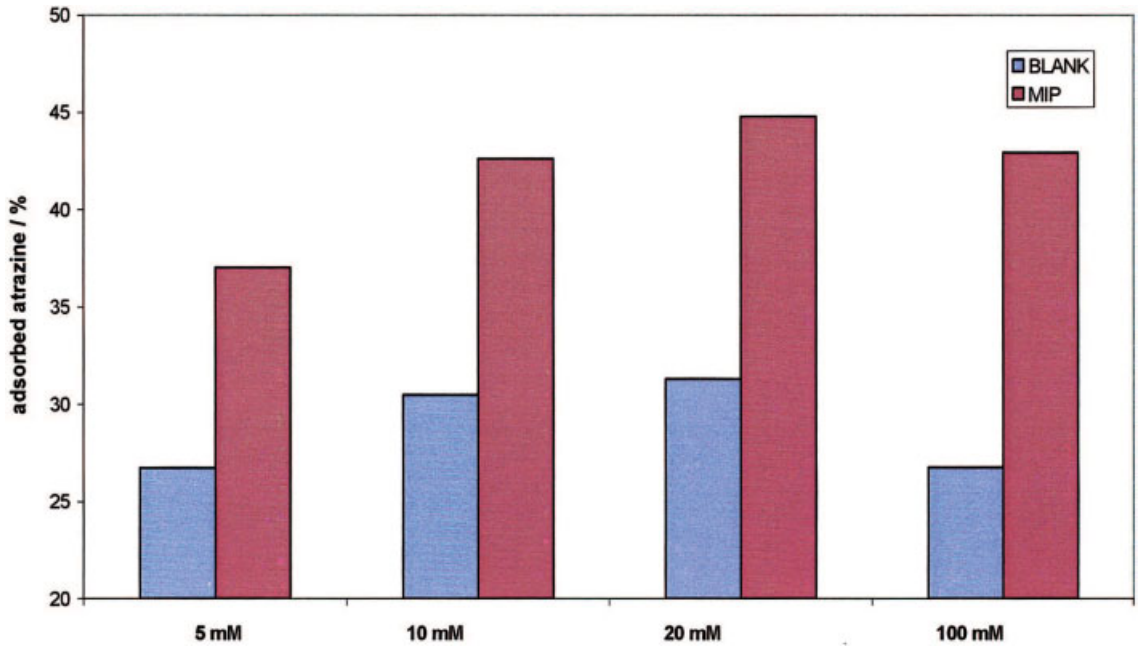


**Figure 5** Binding capacity of thin-layer polymers (300 mM MBAA, 50 mM IA) as a function of buffer concentration ($10^{-5}M$ atrazine, pH 3.5), 10 ml/min. [Color figure can be viewed in the online issue, which is available at www.interscience.wiley.com.]

**TABLE II**
**Atrazin/Simazin Selectivity (S) of Bulk and Thin-Layer Polymers**

| | Bulk particles (%) | Thin-layer polymers (%) |
|---|---|---|
| Blank | 32 | 32 |
| MIP | 37 | 78 |

(bis)ethylamino-1,3,5-triazin]—in the same concentration and under pH and buffer conditions, where the largest imprinting effect had been observed (Table II). Both Blank bulk particles and thin-layer membranes showed the same selectivity (32%) (i.e., atrazine was more strongly bound to the polymers than simazin). An explanation is the higher hydrophobicity of atrazin, expressed by the data lg $K_{ow}$ = 2.61 for atrazin and lg $K_{ow}$ = 2.18 for simazin.[17] Another contribution might be the slightly stronger basic properties of atrazine, which has $pK_a$ = 1.7 as compared with simazine, which has $pK_a$ = 1.62.[17] The MIP bulk particles had a slightly increased selectivity: 37%. However, the selectivity of the thin-layer MIP was much higher: 78%. This could be taken as evidence that molecular recognition of atrazine by the imprinted sites occurred during competitive adsorption under fast SPE conditions.

### Characterization of functional groups

To further characterize the functionality of the polymers—containing the biscarboxylic acid IA as the functional monomer—potentiometric titrations were performed (Figs. 6 and 7). Very different curve shapes were obtained for thin-layer polymers and bulk polymer particles. Whereas the identification of a discrete $pK_a$ value was not possible for the bulk polymers, the titration curves of the thin-layer materials were significantly different from the control experiment without a membrane. They indicated the presence of a well-defined population of carboxylic groups with apparent $pK_a$ values of 6.8 for Blank and 6.6 for MIP.

An exact quantitative determination of carboxylic groups had not been attempted in these experiments. However, it was obvious that the discrepancy between theoretical carboxyl content and acid consumption during titration was also larger for the particles than for the thin-layer composite membranes (cf. Figs. 6 and 7, and Experimental). This could be caused by two different reasons, both linked to the macro- and microstructure of the polymeric materials. The accessibility of the carboxylic groups will be hindered by the porous morphology. For the particles, the kinetics of diffusion into the pores and, especially, through the polymer bulk can significantly delay the proton exchange, whereas for the membranes only, the faster pore diffusion will be involved. The influence of these effects should have been minimized by the very slow titration rate, but—especially for the particles—its impact could not be ruled out completely. On the other hand, the fixation of the functional monomer in a polymer network of inhomogeneous density, flexibility, and mutual proximity of carboxylic acid groups will create different microenvironments with different acidities. For example, an association with another

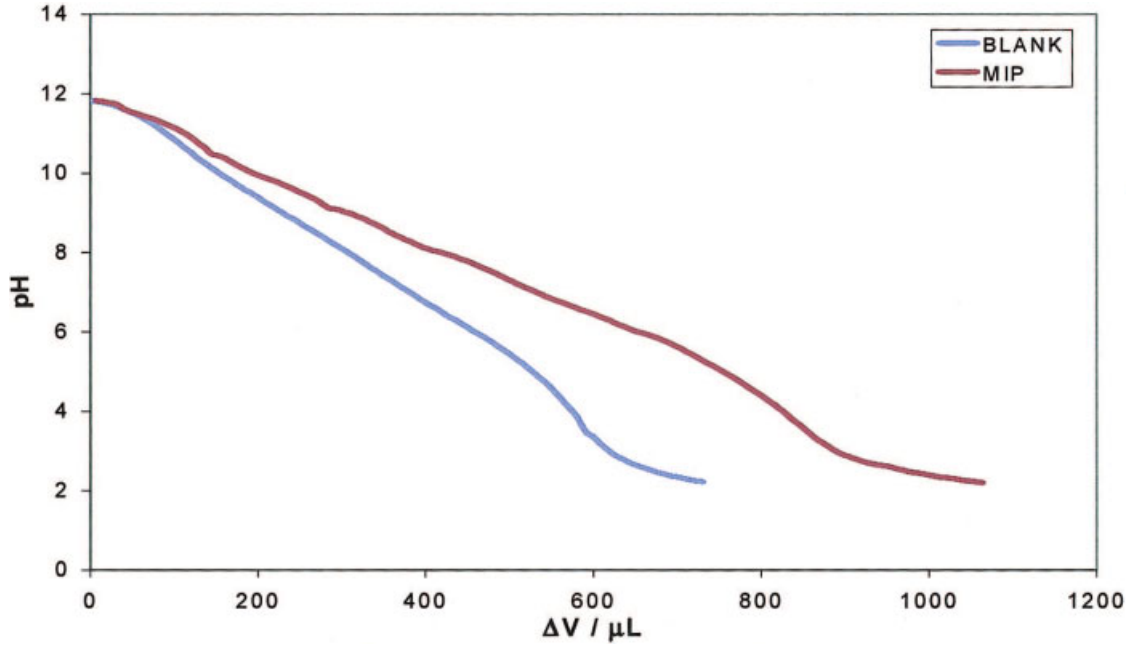


**Figure 6** Titration curve for $pK_a$ determination of bulk polymers (cf. Experimental). [Color figure can be viewed in the online issue, which is available at www.interscience.wiley.com.]

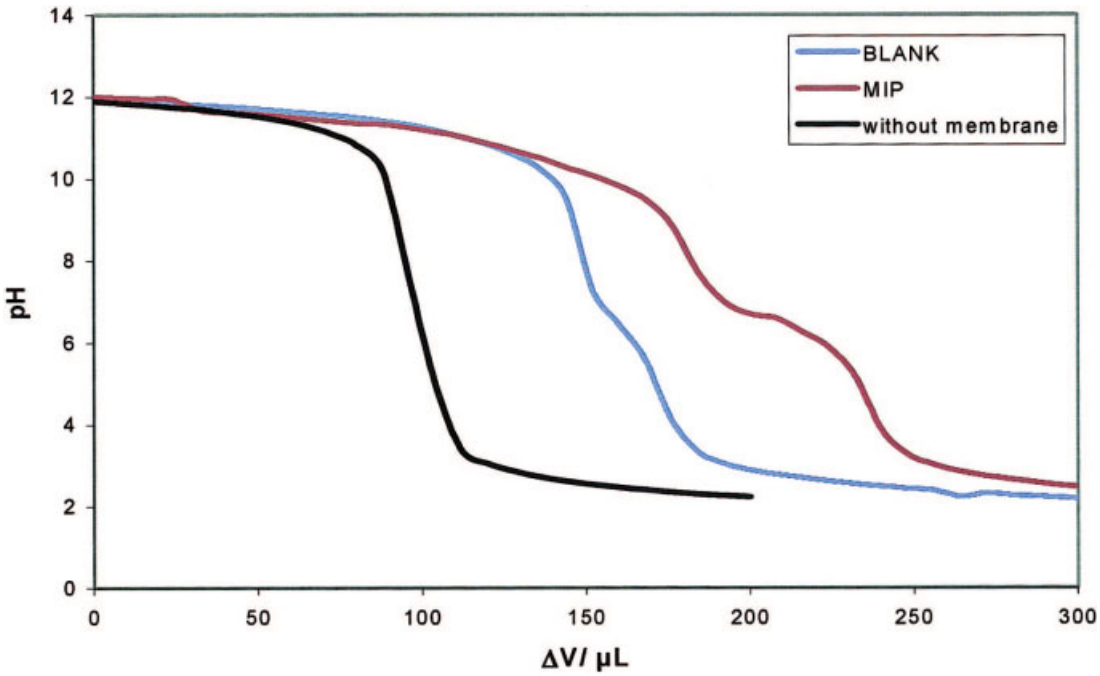


**Figure 7** Titration curve for $pK_a$ determination of thin-layer polymers on PP membranes; control experiment: titration without membrane (cf. Experimental). [Color figure can be viewed in the online issue, which is available at www.interscience.wiley.com.]

carboxylic group and a dissociation of carboxylic groups in close proximity will increase the $pK_a$. Such a thermodynamic effect results in a changed apparent (average) $pK_a$ value of the polymer. Shifts of experimental $pK_a$ values to 8 or even higher had been observed also for other carboxyl-containing highly crosslinked polymers.[18] Obviously, those effects were very pronounced for the bulk particles (cf. Fig. 6). In contrast, most of the carboxylic groups in the thin grafted layers seemed to be located in a much more uniform and less restricted environment (cf. Fig. 7). Nevertheless, the apparent $pK_a$ values of IA were also significantly higher than the known $pK_a$ values in solution: 3.85 and 5.45.[19]

Another important observation was that for the two very different formats—particle and thin-layer—the MIPs seemed to have a larger concentration of titratable carboxylic groups than the corresponding Blanks in both cases. This could be taken as evidence, that their preorganization with the template and subsequent fixation in the polymer network could increase the concentration of well-accessible carboxylic groups. Furthermore, this should be linked to a lower average $pK_a$ value which had indeed been observed (cf. above).

Because the thin-layer polymers showed a higher acidity of carboxylic groups than the bulk particles, a higher polarity of the accessible polymeric binding sites—containing carboxylic groups—could be expected. To prove this assumption, the materials were investigated by using an environmentally sensitive fluorescent probe. Dansyl chloride was selected, which had been reported to bind covalently to carboxylic groups.[20] For dansyl derivatives in different solvents, fluorescence maxima with a systematic dependency on solvent polarity had been observed, from 495 nm (in THF) to 550 nm (in water). Hence, the dansyl probe residing in more unpolar, hydrophobic microenvironment should show a maximum at shorter wavelength as compared with the probe residing in a more polar and thus hydrophilic environment.

The bulk particles showed a fluorescence maximum at shorter wavelength than the composite membranes with the thin-layer polymers (Table III). This difference will be mainly due to the different experimental conditions for measuring the fluorescence (i.e., a particle suspension versus a membrane film). However, the significant differences between MIPs and Blanks of the same format shall be further discussed.

The bulk MIP appeared to be somewhat more polar than the Blank. A possible explanation could be the cooperative influence of the neighboring groups inside of the imprinting cavities pulled together by the template during the complex formation. Of course, the presence of other—less or not organized—carboxylic groups should also be considered, and, consequently, an aver-

**TABLE III**
**Fluorescence Emission Maxima of Dansyl Groups Bound to the Surface of the Polymers**

| | Bulk particles (nm) | Thin-layer polymers (nm) |
|---|---|---|
| Blank | 491 | 513 |
| MIP | 494 | 505 |

age of the information would be obtained. In fact, the observed differences were significant but rather small.

In contrast, the thin-layer MIPs seemed to be significantly more hydrophobic than the Blank polymer layers. This could originate from a contribution of the hydrophobic polypropylene surface to the structure of the imprinted binding sites: A hydrophobic bottom surrounded by fixed carboxylic groups capable of forming a complex with the template could be imagined. In the more randomly polymerized Blanks, IA dimers or clusters held together by hydrogen bonds would perhaps shield the PP surface more efficiently.

### Influence of MIP format, structure, and solution conditions onto binding properties

#### Macroscopic structure effects

In the SPE experiments, the surface area of the bulk particles (15 mg; i.e., 0.9 $m^2$; cf. Table I) was more than three times larger compared to the membranes ($\sim 4$ $cm^2$; corresponding to 13.5 mg,[16] i.e., 0.28 $m^2$; also, a DG of 500 $\mu g/cm^2$ corresponds to 2 mg MIP or Blank). Nevertheless, for the composite membranes much higher binding, relative to the specific surface area of the adsorber material or to the mass of the functional polymer, had been observed (cf. Figs. 2 and 3). A major reason is the high flow rate applied during SPE, which can cause a significant influence of transport rate onto the binding efficiency.

With one membrane (effective area $\sim 4$ $cm^2$ and thickness 155 $\mu$m), the adsorber bed had a volume of $\sim 62$ $\mu$L, and the feed solution would flow through this bed convectively and exclusively via the pore volume ($\sim 47$ $\mu$L; cf. Scheme 1). At a flow rate of 10 mL/min, the average hydrodynamic residence time in the adsorber bed was about 0.3 s. Due to the porous microfiltration membrane structure ensuring very short distances ($< 1$ $\mu$m) to the pore surface where binding takes place, a diffusion resistance for binding will not be critical.[9,21]

For the bulk particles (15 mg), the resulting bed had a diameter of 5.5 mm and a length of $\sim 5$ mm (i.e., a volume of $\sim 120$ $\mu$L). The feed solution will flow through the interparticle volume ($\sim 60$ $\mu$L; cf. Table I) and dispersion into the pore volume will also occur. The particle diameters between 25 and 45 $\mu$m will result in diffusion times of at least 10 s for 50% saturation of the pore volume with the feed solute (using a estimated value for the diffusion coefficient of $8 \times 10^{-10}$ $m^2/s$). This, however, is much longer than the average hydrodynamic residence time of the feed solution in the interparticle volume (0.36 s). The diffusion resistance inside the particles will presumably be even more severe due to the significant swelling of the polyacrylamide-based materials. Note that a limited accessibility had also been a problem during carboxyl titration of the bulk polymers while the thin layers seemed to have a much better accessible structure (cf. Figs. 6 and 7). Finally, attempts to determine static atrazin- or simazin-binding capacities for the bulk materials had yielded very low and thus hardly reproducible values (data not shown). That had also been explained by a significant hindrance for solute diffusion into and equilibration in the bulk materials.

In conclusion, the adsorber capacity of the functional polymer had been used much better in the porous composite membranes than in the bulk particles.

#### Microscopic structure effects

Not only the adsorption capacity (cf. Figs. 2 and 3) but also the binding selectivity of the thin-layer MIPs is much higher than for the bulk MIP particles (cf. Table II). The SPE data under optimal buffer conditions for the bulk materials revealed a very small increase of binding to the MIP as compared to the Blank, and consequently, the imprinting led only to a small increase of selectivity, from 32 to 37%. The magnitude of that effect correlated with a small change of the binding site polarity (cf. Table III). In contrast, for the thin-layer polymers, both binding capacity and selectivity were much improved by imprinting, the latter from 32 to 78% (cf. Table II). However, the fluorescence probe data indicated that the structure of the imprinted sites should have differences compared to the situation in the bulk materials.

The polymer composition of bulk particles and thin layers should be the same. However, whereas the herbicide binding of the bulk functional polyacrylamides will be mainly driven by ionic interactions and hydrogen bonds, perhaps with some contribution of hydrophobic interactions, a strong hydrophobic binding of the triazine herbicides to the PP support material will occur under aqueous conditions. A degree of functionalization of 500 $\mu g/cm^2$ corresponded to an average polymer layer thickness of $\sim 6$ nm (cf. above), which is closed to the critical layer thickness where the PP support surface will not anymore become homogeneously coated. This microscopic inhomogeneity will presumably be facilitated by the polymerization reaction conditions and mechanism. In the early stage of the functionalization, nanometer-sized primary polymer aggregates will be deposited on the membrane surface. The template ionically complexed with the functional monomer will thus also partially be bound to the hydrophobic surface, and a fixation of these nanostructures may lead to the imprinted sites. Hence, an influence of the hydrophobic support as discussed previously[6] could contribute to an enhanced template binding inside of specific imprinted cavities. Here, we assume that the more hydrophobic *and* at the same time more acidic thin MIP layers contain highly structured imprinted sites where also hydrogen bonding can contribute to affinity and selectivity. However, due to the acidity of the functional monomer IA and due to the hydrophilic polyacryl-

amide building blocks, the polymer will be susceptible to changes in pH and buffer.

A variation of the pH value has an influence on the degree of protonation of the carboxylic groups in the polymer. A pH above the $pK_a$ of IA leads to deprotonated carboxylic groups. Below this value, all carboxylic groups are protonated. Whereas for pH values larger than 6.6, ionic interactions will increasingly occur between monomer and template, at a pH 3.5, only hydrogen bonds could be responsible for the template binding. The ionic interactions at higher pH lead to a higher template binding at the expense of a decreased specificity expressed in magnitude of the imprinting effect (cf. Figs. 2 and 3). For the thin-layer polymers, a fixed orientation of the carboxylic groups in the imprinted binding sites had been discussed for the MIPs in contrast to their random arrangement in the Blanks; this may explain the higher binding via long-range ionic interactions for the Blanks at higher pH.

The change in buffer concentration will have an effect on the swelling of the polymer and could have a minor impact onto the ionization of the functional groups in bulk and thin-layer polymers. The first effect especially will lead to a changed geometry of the imprinted binding sites. On the other hand, with increasing buffer concentration, the efficiency of the ionic interactions, which have the largest contribution to nonspecific binding (cf. above), will be reduced. Obviously, the interplay of these two different influences can help to understand the reasons for the optima for the imprinting effect as a function of buffer concentration (cf. Figs. 4 and5). Furthermore, the fixation of the polymer layer to the solid surface of the PP membrane will provide a more rigid structure that is less susceptible to the changes of the solution conditions with an impact on polymer swelling. Therefore, higher buffer concentrations can be used to optimize the imprinting effect.

## CONCLUSIONS

Syntheses of MIP materials in both the traditional—bulk particle—and the novel—thin layer—format were possible from the same reaction mixtures for an *in situ* crosslinking polymerization. Photoinitiation is very versatile to realize similar reaction conditions and to adjust the degrees of monomer conversion most suited for the respective formats. Such photoinitiated syntheses will in the future allow the adaptation of many more of the already established MIP recipes to the preparation of composite materials in the thin-layer MIP format.

The bulk materials, particles from water-compatible polyacrylamides with diameters between 25 and 45 $\mu$m, have a poor performance in fast SPE because of major diffusion transport resistance; nevertheless, an imprinting effect could unambiguously be verified. In contrast, a significantly higher performance of the thin-layer MIPs had been achieved by the separate preparation of a macropore structure (previous membrane formation, here by a manufacturer) and a MIP with the imprinted affinity binding sites. The thin-layer MIPs on hydrophobic PP seem to have a special structure of the binding sites, which is responsible for the affinity and selectivity under aqueous conditions. Further detailed investigations will be necessary towards further improved syntheses and structures of these heterogeneous (organized multifunctional) imprinted sites. This will ultimately enable an optimization of the porous thin-layer MIP composite membranes with the aim to fully explore the application potential of fast SPE, especially for treating large feed volumes.[9,22]

## References


1. Wulff, G. Angew Chem, Int Ed Engl 1995, 34, 1812.
2. Haupt, K.; Mosbach, K. Chem Rev 2000, 100, 2495.
3. Ulbricht, M. Molecularly imprinted polymer films and membranes, in Molecularly Imprinted Materials, Science and Technology; Yan, M.; Ramström, O., Eds.; Marcel Dekker: New York, 2005; pp 455–490.
4. Das, K.; Penelle, J.; Rotello, V. M. Langmuir 2003, 19, 3921.
5. Sulitzky, C.; Rückert, B.; Hall, A. J.; Lanza, F.; Unger, K.; Sellergren, B. Macromolecules 2002, 35, 79.
6. Piletsky, S. A.; Matuschewski, H.; Schedler, U.; Wilpert, A.; Piletskaya, E. V.; Thiele, T. A.; Ulbricht, M. Macromolecules 2000, 33, 3092.
7. Sergeyeva, T. A.; Matuschewski, H.; Piletsky, S. A.; Bendig, J.; Schedler, U.; Ulbricht, M. J Chromatogr, A 2001, 907, 89.
8. Kochkodan, V.; Weigel, W.; Ulbricht, M. Analyst 2001, 126, 803.
9. Ulbricht, M. J Chromatogr, B 2004, 804, 113.
10. Piletsky, S. A.; Day, R. M.; Chen, B.; Subrahmanyam, S.; Piletska, E. V.; Turner, A. P. F. Rational design of MIPs using computational approach, PCT/GB01/00324.
11. Sergeyeva, T. A.; Piletsky, S. A.; Brovko, A. A.; Slinchenko, E. A.; Sergeeva, L. M.; El'skaya, A. V. Anal Chim Acta 1999, 392, 105.
12. Hart, B. R.; Shea, K. J. Macromolecules 2002, 35, 6192.
13. Dirion, B.; Cobb, Z.; Schillinger, E.; Andersson, L. I.; Sellergren, B. J Am Chem Soc 2003, 125, 15101.
14. Lanza, F.; Sellergren, B. Macromol Rapid Commun 2004, 25, 59.
15. Piletsky, S. A.; Piletska, E. V.; Karim, K.; Freebairn, K. W.; Legge, C. H.; Turner, A. F. P. Macromolecules 2002, 35, 7499.
16. Borcherding, H.; Hicke, H. G.; Jorcke, D.; Ulbricht, M. Ann NY Acad Sci 2003, 984, 470.
17. (a) Montgomery, J. H. Agrochemical Desk Reference: Environmental Data; Lewis Publishers: Ann Arbor, 1993; (b) Tomlin, C. D. S. The Pesticide Manual; BCPC: Berkshire, 2000; (c) Bouchard, D. C.; Lavy, T. L. J Environ Qual 1985, 14, 181.
18. Sellergren, B.; Shea, K. J. J Chromatogr, A 1993, 654, 17.
19. Merkli, A.; Heller, J.; Tabatabay, C.; Gurny, R. J Controlled Release 1995, 33, 415.
20. Bartzatt, R. J Biochem Biophys Methods 2001, 47, 189.
21. Roper, D. K.; Lightfoot, E. N. J Chromatogr, A 1995, 702, 3.
22. Hennion, M. C. J Chromatogr, A 1999, 856, 3.